J. Physiol. (1987), **387**, *pp.* 227–250
With 12 *text-figures*
Printed in Great Britain

CONDUCTANCE AND KINETICS OF DELAYED RECTIFIER POTASSIUM CHANNELS IN NODAL CELLS OF THE RABBIT HEART

BY TOHRU SHIBASAKI

From the National Institute for Physiological Sciences, Myodaiji, Okazaki 444, Japan

(*Received 14 July 1986*)

SUMMARY

1. The delayed rectifier K^+ current (I_K) of single pace-maker cells from the sino-atrial node and the atrioventricular node of the rabbit heart was investigated using the whole-cell and cell-attached configurations of the patch-clamp technique.

2. The activation kinetics of the macroscopic I_K were not altered by varying the extracellular K^+ concentration ($[K^+]_o$) between 5·4 and 150 mM. The amplitude of the tail current of I_K, however, was about 10-fold larger at a $[K^+]_o$ of 150 mM than that at a $[K^+]_o$ of 5·4 mM.

3. By using a high-$[K^+]_o$ solution, inward single-channel currents were observed on repolarization from potentials positive to −40 mV. The current–voltage (I–V) relation was linear over the negative potential range and the reversal potential estimated by extrapolating the I–V curve was shifted by about 60 mV for a 10-fold increase in $[K^+]_o$, indicating that the channel was highly selective for K^+.

4. The single-channel conductance was 11·1 pS at a $[K^+]_o$ of 150 mM and varied in proportion to the square root of $[K^+]_o$. The total number of channels was estimated as approximately 1000 per cell (0·7/μm^2). On repolarization, the averaged single-channel current disappeared with a time constant similar to that of the macroscopic tail current of I_K.

5. At potentials between −50 and −100 mV, the open and closed times of the single channel fitted well with single-exponential and biexponential distributions, respectively. As the membrane was progressively depolarized, the open time was shortened while the closed time was prolonged, suggesting a decrease of open probability. These changes were in the opposite direction to those expected from the delayed rectifier K^+ current which progressively increases in magnitude at more positive potentials.

6. At the beginning of the macroscopic tail current, a transient increase of the inward current was found to precede the time-dependent decrease. This rapid initial change can be attributed to a quick removal of inactivation of I_K which had occurred during the depolarizing pulse. This inactivation gate of the channel has very fast kinetics and could be responsible for the inward-going rectification observed in the 'fully activated' I_K.

Present address: 2nd Department of Internal Medicine, Gifu University School of Medicine, Tsukasamachi, Gifu 500, Japan.

INTRODUCTION

In cardiac pace-maker cells, a slow decay of the K^+ outward current (I_K) has been interpreted as one of the major causes of pace-maker depolarization (for reviews, see Irisawa, 1978; Brown, 1982). This current system has been extensively analysed in the mammalian sino-atrial node and the atrioventricular node (Noma & Irisawa, 1976; DiFrancesco, Noma & Trautwein, 1979; Brown, Kimura & Noble, 1982; Kokubun, Nishimura, Noma & Irisawa, 1982) as well as in the frog sinus venosus (Brown, Giles & Noble, 1977). Recently, the results obtained with these multicellular specimens have been largely confirmed in single pace-maker cells isolated from both mammalian and amphibian nodal tissues (Nakayama, Kurachi, Noma & Irisawa, 1984; Giles & Shibata, 1985).

The detailed properties of I_K, however, have not yet been clarified. For example, in macroscopic current analysis, the degree of inward rectification in the 'fully activated' current–voltage relation varies among different investigators, and the mechanism of the rectification has not been elucidated. The outward tail current on repolarization has been found to have two exponential components, but whether this is due to two separate classes of channels remains unknown. These problems may be resolved if the single-channel current is recorded by the patch-clamp technique (Hamill, Marty, Neher, Sakmann & Sigworth, 1981).

In the present experiments, single-channel currents of I_K were recorded in a cell-attached patch of single pace-maker cells of rabbit sino-atrial and atrioventricular nodes using a solution of high extracellular K^+ concentration ($[K^+]_o$). Based on the single-channel current data obtained, the kinetics of the macroscopic I_K is described.

METHODS

Preparations. The method of isolating single nodal cells from the rabbit heart with collagenase was as described in detail elsewhere (Taniguchi, Kokubun, Noma & Irisawa, 1981; Kakei & Noma, 1984; Nakayama *et al.* 1984). Briefly, the heart was dissected from a rabbit of 1·0–1·5 kg body weight, mounted on a Langendorff apparatus and perfused with a nominally Ca^{2+}-free Tyrode solution containing 0·04 % (w/v) collagenase (Sigma, type I). After 40 min of collagenase treatment, the heart was perfused with high-K^+, low-Cl^- solution (Taniguchi *et al.* 1981; Isenberg & Klöckner, 1982). A small piece of tissue (1 × 1 mm) dissected from the endocardial side of the sino-atrial or the atrioventricular node was teased in a recording chamber (0·9 ml) filled with Tyrode solution to isolate single cells. After the cells had settled at the bottom of the chamber, they were perfused with Tyrode solution at a rate of 2–5 ml/min. Although the isolated nodal cells were spindle shaped in the high-K^+, low-Cl^- solution, they became round within an hour in the Tyrode solution. Since the myofibrils of the nodal cells are little organized, the cells would be able to assume the round shape without changing the volume (Nakamura, Hama, Asai & Irisawa, 1986). About 10–30 % of cells of 15–30 μm in diameter had a smooth surface and beat regularly at a frequency of 150–260/min. The round cells were used in the present study, and cells with a rough surface or irregular beat were discarded. The experiments were carried out at 36–37 °C.

Solutions. The compositions of the external and internal solutions for whole-cell or single-channel current recordings are listed in Table 1 and Table 2, respectively. In the whole-cell configurations, D600 (Knoll) was employed to block the calcium current. Although it had been reported that D600 made the cell membrane leaky and slightly decreased the amplitude of I_K (see Nakayama *et al.* 1984), application of cyclic AMP in the pipette solution prevented these effects. In preliminary experiments, it was found that cyclic AMP did not modify the activation or deactivation process of I_K, as reported by Noma, Kotake & Irisawa (1980) who applied adrenaline. Acetylcholine (ACh,

TABLE 1. Composition of solutions for whole-cell current recordings (mM)

	External*				
	NaCl	NaH_2PO_4	KCl	$CaCl_2$	$MgCl_2$
Tyrode solution	143	0·33	5·4	1·8	0·5
50 mM-K^+ solution	98·4	0·33	50	1·8	0·5
150 mM-K^+ solution	—	—	150	1·8	0·5

	Internal†					
	K aspartate	KCl	$MgCl_2$	EGTA	ATP	CrP
150 mM-K^+ solution	90	20	1	5	5	10

The pH of the solutions was adjusted to 7·4 with 5 mM-HEPES–KOH, except in Tyrode and 50 mM-K^+ solutions which were adjusted with 5 mM-HEPES–NaOH. The external solution contained 5·5 mM-glucose. The liquid junction potential (−13 mV) between the 150 mM-K^+ internal solution and Tyrode solution was corrected (Matsuda & Noma, 1984).

ATP: adenosine 5′-triphosphate (dipotassium salt, Sigma).

CrP: creatine phosphate (dipotassium salt, Calbiochem–Behring Corp). * and † contained 1×10^{-6} M-D600 and 1×10^{-4} M-cyclic AMP, respectively.

TABLE 2. Composition of solutions for single-channel current recordings (mM)

	External*				
	NaCl	NaH_2PO_4	KCl	$CaCl_2$	$MgCl_2$
20 mM-K^+ solution	128·4	0·33	20	1·8	0·5

	In pipette (internal)†			
	KCl	NaCl	$CaCl_2$	$MgCl_2$
50 mM-K^+ solution	50	98·4	1·8	0·5
100 mM-K^+ solution	100	50	1·8	0·5
150 mM-K^+ solution	150	—	1·8	0·5
200 mM-K^+ solution	200	—	1·8	0·5
300 mM-K^+ solution	300	—	1·8	0·5

The pH of the solutions was adjusted to 7·4 with 5 mM-HEPES–KOH, except in 20 mM-K^+ (external), 50 mM-K^+ and 100 mM-K^+ (internal) solutions which were adjusted with 5 mM-HEPES–NaOH. The external solution contained 5·5 mM-glucose. * and † contained 2×10^{-7} M-ACh and 1×10^{-7} M-atropine, respectively.

2×10^{-7} M) was temporally superfused to suppress spontaneous firing of the nodal cells when attaching the electrode to the cell. In case of cell-attached patch recording, ACh was continuously perfused and atropine in the pipette was used to suppress the ACh-sensitive K^+ channel (Sakmann, Noma & Trautwein, 1983; Soejima & Noma, 1984). The average resting potential of the nodal cells in 20 mM-extracellular K^+ solution containing ACh was -39 ± 3 mV for thirty-three cells, as determined after the single-channel current measurements. The membrane potential was obtained as the difference between −40 mV (the resting potential) and the pipette potential.

Recording techniques. The whole-cell and cell-attached patch-clamp methods were essentially the same as described by Hamill *et al.* (1981). The resistance of the fire-polished glass pipette electrode was 2–5 MΩ with tip diameters of 2–3 μm for whole-cell current recordings, and 10–20 MΩ with tip diameters of 0·5–1·5 μm for single-channel current recordings. The shank of the pipette was coated with silicon near the tip for the single-channel current recordings.

For the whole-cell current recordings, a current–voltage converter with a feed-back resistor of 100 MΩ was employed (for details, see Matsuda & Noma, 1984). Single-channel currents were

recorded with a List EPC-7 amplifier. The current and voltage signals were stored in a video cassette recorder (Victor, BR6400) using a PCM converter system (NF, RP-882). After the recorded currents had been low-pass filtered at 1 kHz with a Bessel-type active filter (48 dB/oct., NF, FV-625A), they were sampled with a 12-bit analog-to-digital converter at an interval of 0·2–3 ms (particularly 0·2 ms in single-channel current recordings) for analysis with a computer (HITAC E-600).

In the single-channel current analysis, capacity and leakage currents were removed digitally by averaging traces that included no channel openings and subtracting the resultant average current from each trace. The initial 2 ms of the test pulse was omitted from the analysis because of capacitive artifacts. The points of the beginning and end of the channel opening and the unit amplitude were estimated by eye on the digitized original records and idealized as square-pulse events. Membrane patches showing only one I_K channel activity and no overlaps of the unitary current throughout the entire period of recording were subjected to analysis of the kinetics. All results are given as the mean ± S.D.

RESULTS

Dependence of whole-cell I_K on extracellular K^+

There has been no previous report on the single-channel analysis of I_K in cardiac pace-maker cells. This may be accounted for by a small single-channel conductance, low opening probability or quick run-down of the channel activity. For this reason, the author first sought conditions under which I_K could have a large conductance in the whole-cell clamp mode. Since the conductance of K^+ channels generally increases on elevating $[K^+]_o$, I_K was investigated at high $[K^+]_o$.

When $[K^+]_o$ was 5·4 mM, the amplitude of the outward current increased progressively in response to progressively larger depolarizing test pulses and so did that of the outward tail current upon subsequent repolarization to −43 mV (Fig. 1). The outward tail current almost reached a saturation level as the test pulse was increased more positive to −13 mV, but the magnitude of the current tail was very small and never exceeded 50 pA. When $[K^+]_o$ was increased from 5·4 to 50 mM, the maximum value of the tail current upon repolarization to −43 mV became less than 30 pA (not shown in the Figure) because −43 mV is very close to the K^+ equilibrium potential of −29 mV at a $[K^+]_o$ of 50 mM, where the internal solution contains 150 mM-K^+ ($[K^+]_i$). Repolarization to −73 mV in a $[K^+]_o$ of 50 mM, however, made the tail current inward (Fig. 1), and the maximum current amplitude became as large as about 300 pA. When $[K^+]_o$ was further increased to 150 mM, even larger tail currents were recorded.

During depolarization positive to 7 mV, a slow decay of the outward current was consistently observed following the initial activation phase of the outward current. In addition, a transient inward deflexion of the current or a 'hook' was observed in higher time-resolution records (inset to Fig. 1) at the beginning of the tail current. Mechanisms of these current changes will be examined later.

The amplitude of the tail current was measured at three different $[K^+]_o$ levels in the same cell (Fig. 2*A*). The outward tail current could be separated into two exponential components as had been reported previously (DiFrancesco *et al.* 1979; Nakayama *et al.* 1984). In the present study, the amplitude of the tail current was measured as the difference between the initial peak and the current level 1 s after the onset of repolarization. This was done only for practical purpose, especially because the inward tail current showed nearly single-exponential decay. I_K started to be activated at −50 mV and was fully activated at about +10 mV, regardless of

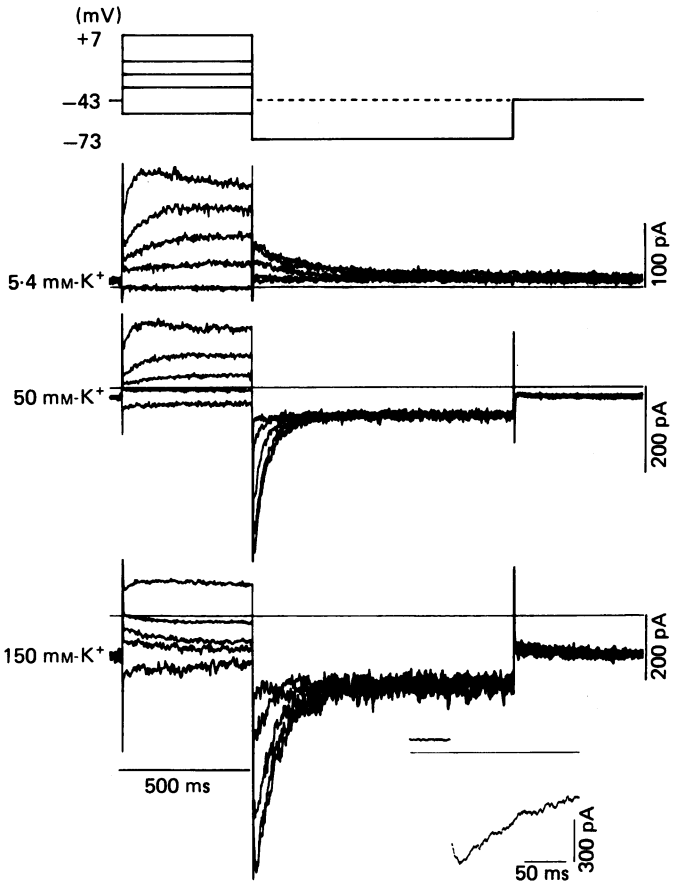

Fig. 1. Voltage-dependent activation of I_K at a $[K^+]_o$ of 5·4, 50 and 150 mM in the same cell. The top panel shows the experimental paradigm, where various test pulses of 0·5 s duration were applied and the membrane was subsequently repolarized to −43 mV at a $[K^+]_o$ of 5·4 mM or to −73 mV at a $[K^+]_o$ of 50 and 150 mM. Currents in response to test pulses (−53, −33, −23, −13 and +7 mV) from a holding potential of −43 mV are superimposed. Outward current tails were observed at a $[K^+]_o$ of 5·4 mM. At a $[K^+]_o$ of 50 and 150 mM, the current tails were inward, since the reversal potential for K^+ was calculated as −29 mV in 50 mM-extracellular K^+–150 mM-intracellular K^+ and 0 mV in 150 mM-extracellular K^+–150 mM-intracellular K^+. Activation of the hyperpolarization-activated inward current (I_f or I_h) was not significant in this specimen. The inset shows a faster time-resolution record upon repolarization from +7 to −73 mV in a $[K^+]_o$ of 150 mM.

different $[K^+]_o$. In thirteen cells, the average amplitude of the tail current was 0·06±0·04 nA (at −43 mV; $n = 13$), 0·29±0·12 nA (at −73 mV; $n = 9$) and 0·61±0·20 nA (at −73 mV; $n = 10$) in $[K^+]_o$ levels of 5·4, 50 and 150 mM, respectively. The result indicates that it may be possible to record single-channel currents of I_K at high $[K^+]_o$, but not at a $[K^+]_o$ of 5·4 mM.

In order to evaluate the activation curves at different $[K^+]_o$ levels, the amplitudes of the tail currents were normalized by taking the maximum value as unity (Fig. 2*B*).

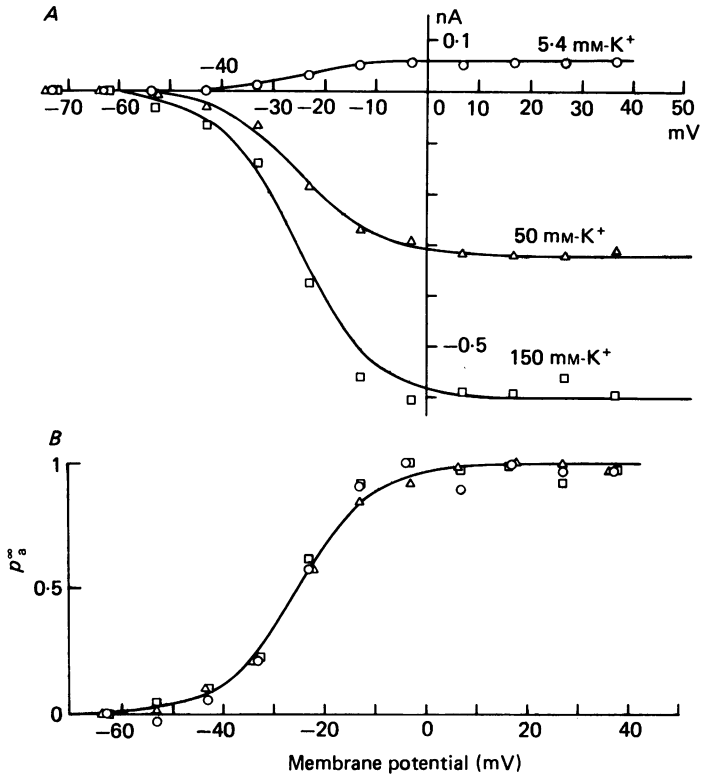

Fig. 2. *A*, current–voltage relation of the I_K tail current in different $[K^+]_o$ solutions. Data were obtained from the same cell as in Fig. 1. The amplitude of the tail current (at $t = 0$) was measured by extrapolating the time course towards the beginning of the repolarizing pulse with respect to the current level at 1 s after the onset of repolarization. *B*, steady-state activation curve for I_K at three different $[K^+]_o$ values. The amplitudes were normalized by taking the maximum value of p_a^∞ as unity, where p_a^∞ is the steady-state open probability of the activation gate. The smooth curve is the least-squares fit of eqn. (1) with $E_h = -25{\cdot}1$ mV and $s = 7{\cdot}4$ mV. ○, △ and □ indicate 5·4, 50 and 150 mM-extracellular K^+, respectively for both *A* and *B*.

The activation curves for I_K at the three different values of $[K^+]_o$ were superposable and fitted well with a sigmoidal function, which could be given by

$$p_a^\infty = \left(1 + \exp\frac{E_h - E}{s}\right)^{-1}, \quad (1)$$

where p_a^∞ is the open probability of the activation gate in the steady state, and E is the membrane potential in millivolts. The slope factor (s) and the membrane potential with half-maximum activation (E_h) were 7·4 mV and −25·1 mV, respectively. The time constant of the I_K tail at −63 mV did not reveal any statistically significant difference between a $[K^+]_o$ of 5·4 mM (156 ± 21 ms; $n = 5$) and 150 mM (173 ± 37 ms; $n = 5$) (for details, see Fig. 7). This finding indicates that the activation kinetics of I_K is dependent on the membrane potential but is independent of $[K^+]_o$. On the basis of these results, single-channel currents underlying the inward tail currents in high-$[K^+]_o$ solution were studied in the following section.

Single-channel current of I_K in the cell-attached patch

The single-channel current records in Fig. 3*A* were obtained with the 'gigaseal' patch pipette containing 100 mM-K^+. The membrane potential was first held at 0 mV and then hyperpolarized to different potentials. Corresponding to the tail of I_K, the

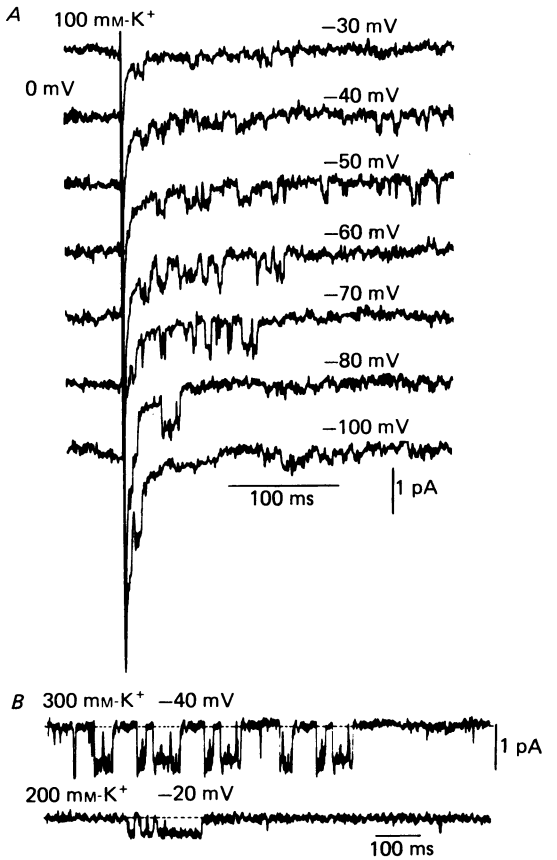

Fig. 3. Records of single-channel currents. *A*, the patch membrane was held at 0 mV and hyperpolarizing step pulses were given to the various potentials indicated. The leakage current was subtracted from each trace. No detectable unitary currents could be seen at the holding potential, but current steps of uniform amplitudes were seen more at the beginning of the negative pulse. *B*, single-channel current records in the steady state at −40 mV with a patch electrode containing 300 mM-extracellular K^+ (upper trace), and −20 mV with 200 mM-extracellular K^+ (lower trace). Inward currents are downward.

opening of a class of channels was observed as inward unitary currents upon hyperpolarization of the patch membrane, while there were no apparent signs of channel opening at 0 mV.

At potentials negative to −80 mV, single-channel currents, the amplitude of which was larger than 1 pA, appeared at the beginning of the pulse, and the events disappeared within 100 ms after the onset of the pulse. As the hyperpolarizing potential became less negative, the unit amplitude of the current decreased and the

channel events frequently persisted for more than 200 ms. In Fig. 3*B*, when 200 mM-K^+ pipette solution was used, single-channel currents of 0·35 pA were seen in the steady state at −20 mV. Increasing $[K^+]_o$ to 300 mM increased the single-

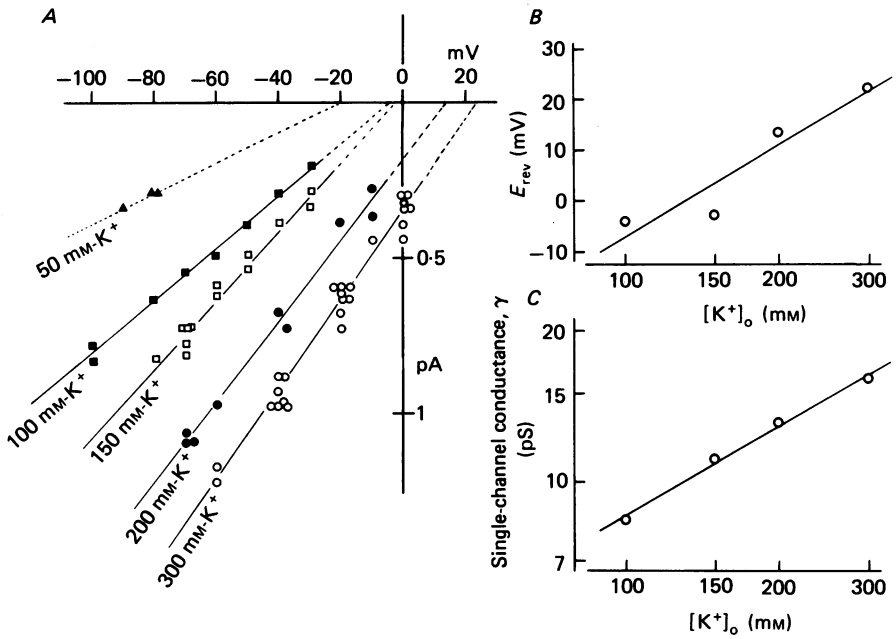

Fig. 4. *A*, relation between the unit amplitude of single-channel currents and the membrane potential at different $[K^+]_o$ values. The $[K^+]_o$ in the pipette is indicated on each line. The single-channel conductance (γ) was measured from the slope of the regression line which was fitted by the least-squares method for each $[K^+]_o$. The values of γ at 100, 150, 200 and 300 mM-extracellular K^+ were 8·4, 11·1, 13·1 and 14·7 pS, respectively. The reversal potential (E_{rev}) was defined as the intersect of each regression line on the abscissa. *B*, E_{rev} as a function of $[K^+]_o$. The values were plotted against the logarithm of the K^+ concentration in the pipette solution and fitted a straight line with a slope of 60 mV per 10-fold change in $[K^+]_o$. *C*, single-channel conductances as a function of $[K^+]_o$. The values of γ were plotted against the K^+ concentration in the pipette solution. In double-logarithmic coordinates, the data points could be fitted to a straight regression line having a slope of 0·59.

channel currents to 1 pA at −40 mV. Although the channel events appeared in the steady state, they tended to decline slowly, probably because of run-down phenomena. In the potential range between −100 and +20 mV, outward single-channel currents could not be detected regardless of $[K^+]_o$.

The current–voltage (*I–V*) relations measured from the inward single-channel currents were linear with different $[K^+]_o$ values (Fig. 4*A*). Increasing $[K^+]_o$ increased the channel conductance. The reversal potential, estimated by extrapolation of the *I–V* curve, shifted in the right direction as $[K^+]_o$ was increased. Plots of the reversal potential against the logarithm of the K^+ concentration in the pipette solution gave a slope of 60 mV for a 10-fold increase in $[K^+]_o$ (Fig. 4*B*). This result indicates that the unitary current in the present experiments was carried by K^+.

At potentials negative to the reversal potential, the single-channel conductance was voltage independent, as shown by the linear *I–V* relations in Fig. 4*A*. Fig. 4*C* illustrates the relationship between the single-channel conductance (γ) in pS and $[K^+]_o$ in mM, where γ is given by

$$\gamma = 0{\cdot}58\,[K^+]_o^{0{\cdot}59}. \quad (2)$$

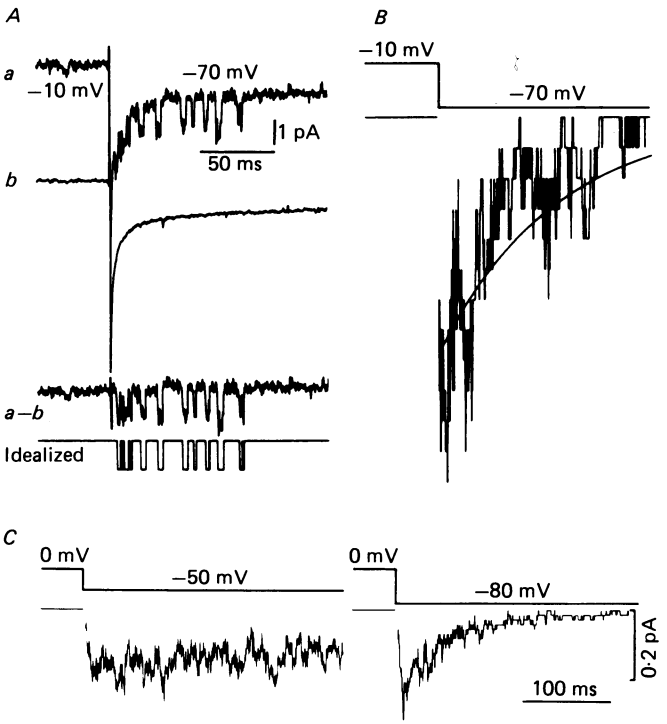

Fig. 5. Reconstruction of the macroscopic current from single-channel currents. *A*, original single-channel currents recorded at −70 mV stepped from a holding potential of −10 mV. To remove the capacitive and leakage currents, current traces having no channel openings were averaged, as shown in *b*, and the averaged curve was subtracted from each original record (*a*−*b*). The idealized record (bottom trace) was then obtained. $[K^+]_o$ was 200 mM. *B*, averaging forty-eight idealized traces, from the same patch membrane as in *A*, gave the ensemble average current, having a decaying time constant of 79 ms on repolarization to −70 mV. *C*, time courses of deactivation of the averaged current from single-channel currents at a $[K^+]_o$ of 100 mM. The patch membrane was hyperpolarized from 0 to −50 mV (left) or to −80 mV (right), respectively.

A similar value to the 0·59th power has been obtained in the case of the inward rectifier K^+ channel (Hagiwara & Takahashi, 1974; Fukushima, 1982; Sakmann & Trube, 1984*a*) and the ACh-sensitive K^+ channel (Sakmann *et al.* 1983). Eqn. (2) yields a single-channel conductance of 1·6 pS in Tyrode solution (with a $[K^+]_o$ of 5·4 mM). Assuming that the *I–V* relation obeys the constant-field equation, the permeability of this K^+ channel will be $2{\cdot}0 \times 10^{-14}$–$2{\cdot}3 \times 10^{-14}$ cm³/s in a $[K^+]_o$ of 5·4–300 mM. These values are similar to the permeability of the delayed rectifier K^+ channel in squid axons ($2{\cdot}85 \times 10^{-14}$ cm³/s, Conti & Neher, 1980).

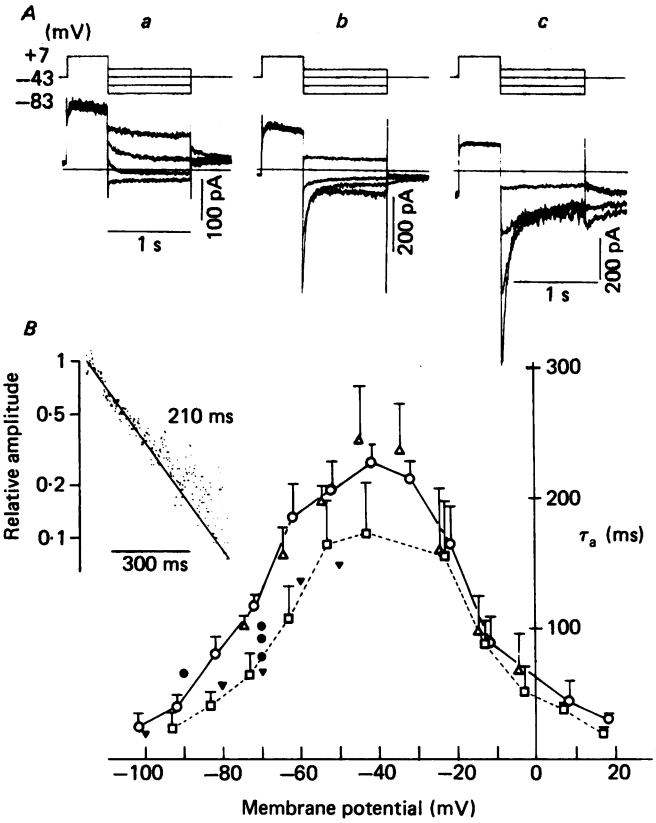

Fig. 6. *A*, voltage dependence of the time course of deactivation of I_K. The top panel shows the experimental paradigm, where the membrane potential was initially depolarized to +7 mV from a holding potential of −43 mV, and various test pulses of 1 s duration were subsequently applied. The lower panel gives the corresponding current tracings. In *Aa*, the experiment was carried out at a $[K^+]_o$ of 5·4 mM, whereas in *Ab* and *Ac* the levels of $[K^+]_o$ were 50 and 150 mM, respectively. *B*, relationship between the time constant of the activation gate (τ_a) and the membrane potential. Open symbols indicate data from whole-cell currents and filled symbols, those from ensemble averages of single-channel currents. $[K^+]_o$ (in mM): △, 5·4; □, 50; ○, 150; ▼, 100; ●, 200. At potentials positive to −30 mV, the time constant was measured from the time course during depolarization (Fig. 1) or from the envelope curve (Fig. 9). The sample number of measurements was 4–6, and the bars denote the mean+S.D. The time constant of the tail current in the whole-cell recording was measured with respect to the current level at 1 s after the onset of repolarization, while the time constant in the ensemble average currents was measured with respect to the current level at 300 ms after the onset of repolarization. The inset shows the deactivation time course of macroscopic I_K at −60 mV and a $[K^+]_o$ of 150 mM, which fitted well to a single-exponential curve.

Time course of the ensemble average current and the activation–deactivation process of the whole-cell I_K

To confirm that the unitary current belongs to the delayed rectifier K^+ channel, the ensemble average current was constructed from the single-channel traces at −70 mV (Fig. 5*A* and *B*). The ensemble average current obtained by summing the

idealized records in Fig. 5*B* exhibits a configuration similar to the I_K tail current. In four examples, the time constant of the current decay was 85 ± 16 ms at -70 mV, which was not greatly different from that of the I_K tail obtained in the whole-cell recordings (118 ± 7 ms at -73 mV; $n = 5$). The decay of the ensemble average current became faster as the potential became more negative from -50 mV to -80 mV as shown in Fig. 5*C*. This phenomenon also resembles the whole-cell I_K.

The relation between the time constant of current decay and the membrane potential with various $[K^+]_o$ solutions is summarized in Fig. 6 for both the whole-cell current (open symbols) and the ensemble average current (filled symbols). The time constant of the macroscopic current decay formed a bell-shaped function to which that of the average current coincided reasonably well. The time constants of the macroscopic I_K decay were similar between $[K^+]_o$ values of 5·4 and 150 mM, indicating that the kinetics of the activation gate is independent of $[K^+]_o$, so confirming the results in Fig. 2*B*. The time constants at a $[K^+]_o$ of 50 mM showed slightly smaller values than those at $[K^+]_o$ values of 5·4 and 150 mM. A possible reason for this will be given in the Discussion. The voltage dependence of the time constant of activation or deactivation can be simulated by the following empirical equation:

$$\tau_a^{-1} = 17{\cdot}0 \exp(0{\cdot}0398E) + 0{\cdot}211 \exp(-0{\cdot}0510E), \quad (3)$$

where τ_a is the time constant of an activation gate in seconds and E is the membrane potential in millivolts.

Since the unitary current was highly selective for K^+, and the time course of the ensemble average current coincided with that of the macroscopic I_K, it can be concluded that the unitary current recorded in this experiment was responsible for the macroscopic I_K.

Time constants of the open time and closed time

To analyse the kinetics of the single-channel current, open- and closed-time histograms were constructed from the idealized records as shown in Fig. 5*A*. Fig. 7*A* shows the results obtained by giving repetitive hyperpolarizing pulses of 300 ms to -60 mV from a holding potential of $+20$ mV. The open-time histogram fitted well with a single-exponential curve having a time constant of 2·5 ms, whereas the closed-time histogram fitted two exponentials comprising a fast and a slow component with time constants of 0·7 and 17·6 ms, respectively. These three time constants, viz. τ_{open}, τ_{slow} and τ_{fast}, were plotted as a function of the membrane potential (Fig. 7*B*). The time constants can be said to be markedly shorter than those expected from the deactivation time course of the macroscopic tail current. In the potential range between -100 and -50 mV, τ_{open} tended to become shortened at less-negative potentials while τ_{slow} was prolonged and τ_{fast} showed no significant change. These results suggest that the open probability of this channel decreased as the membrane depolarized. This change would appear to be in the opposite direction to the delayed rectifier K^+ current which consistently increases at more positive potentials. This discrepancy cannot be resolved by the conventional concept that I_K has only an activation gate: it therefore requires the presence of another gate, viz. an inactivation gate. Proof that there is indeed an inactivation gate of I_K will be provided below in the whole-cell experiments.

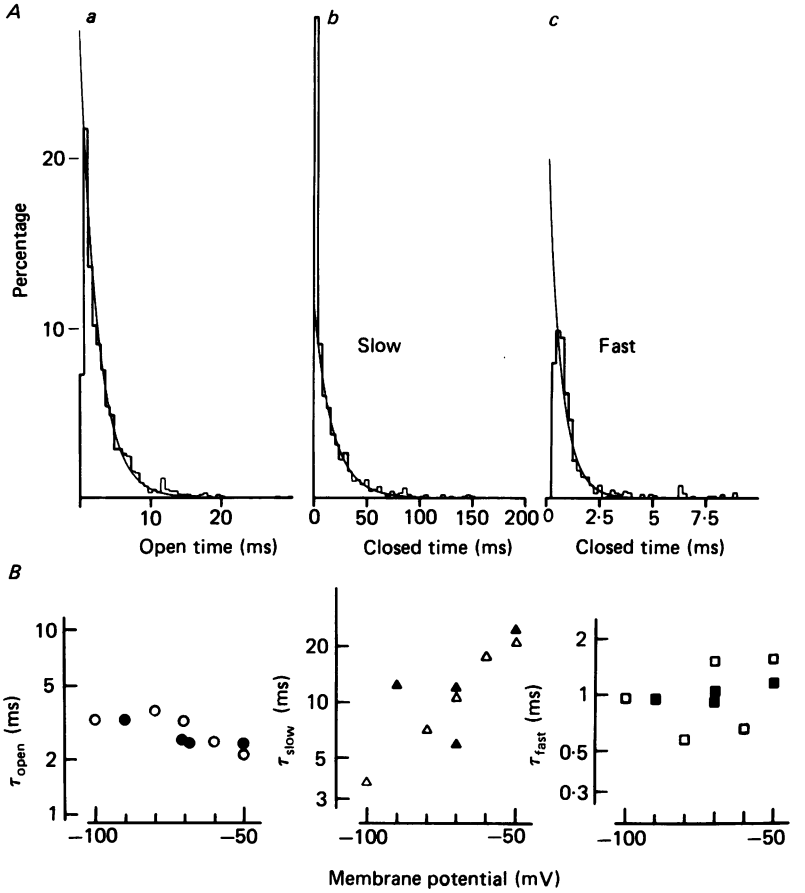

Fig. 7. *A*, distribution of open and closed times during a series of hyperpolarizing pulses (−60 mV) of 300 ms in duration and 0·5 Hz in frequency from a holding potential of +20 mV. The total sample number was 1020. The histogram of the open time (*a*) was fitted by a single exponential with a time constant of 2·5 ms (τ_{open}) using a bin width of 0·6 ms. The histogram of the closed time (*b*) was obtained using a bin width of 4 ms. The slow component fitted well with a time constant (τ_{slow}) of 17·6 ms. Extrapolation of the exponential curve to time zero showed an excess of events with shorter closed times. Subtracting the slow component from the histogram yielded the fast component (*c*) with a time constant (τ_{fast}) of 0·7 ms using a bin width of 0·2 ms. The K^+ concentration in the pipette was 100 mM. *B*, time constants for the distributions of the open and closed times (τ_{slow} for the slow component and τ_{fast} for the fast component) at various membrane potentials. Open symbols indicate a $[K^+]_o$ of 100 mM in the pipette and filled symbols, a $[K^+]_o$ of 200 mM.

Quick removal of fast inactivation

As mentioned earlier, a 'hook' was observed at the beginning of the I_K deactivation process (inset to Fig. 1). In Fig. 8*A*, the initial phase of the tail current at −73 mV in the presence of a $[K^+]_o$ of 150 mM was examined at higher time resolution. After depolarization to −33 mV, the tail current appeared to consist of only a phase of deactivation. After a pre-pulse to −23 mV, however, the tail current on repolariz-

ation exhibited a small 'hook', which became more prominent after a pre-potential of +17 mV. To delineate the initial current change from the deactivation process more clearly, the current trace was digitally divided by a curve which had the time

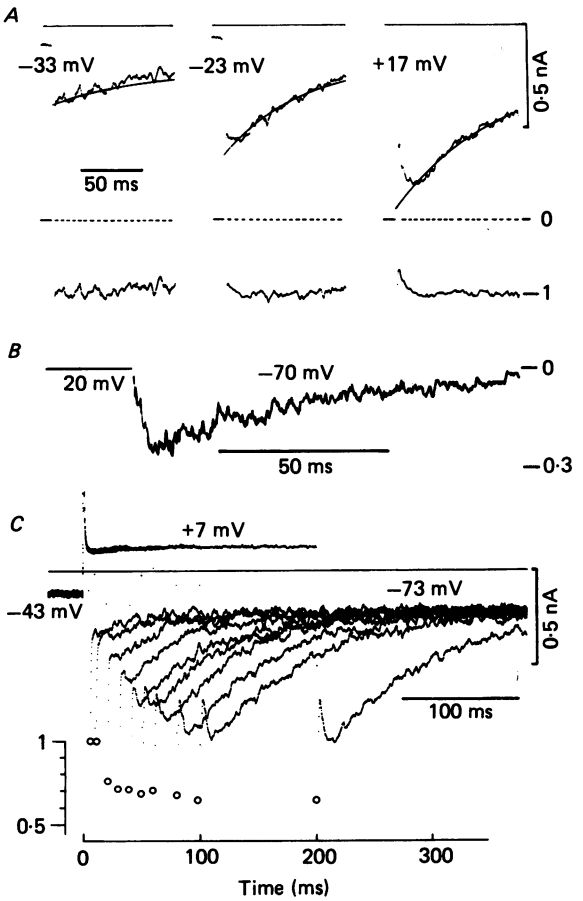

Fig. 8. A fast inactivation gate of I_K. *A*, in the upper row, the membrane potentials were clamped back to −73 mV from −33, −23 and +17 mV, respectively. In the lower row, the ratios of the original current trace to time course of deactivation are shown as a function of time. $[K^+]_o$ was 150 mM. *B*, open-state probability of one single channel as a function of time, obtained from 156 idealized single-channel current traces. The repolarizing pulse was given from a holding potential of +20 mV to −70 mV. $[K^+]_o$ was 200 mM. *C*, inactivation process of the macroscopic I_K during depolarization. The membrane was first depolarized from a holding potential of −43 mV to +7 mV for various durations and then repolarized to −73 mV. In the lower row, plots are the ratios of the quasi-instantaneous current level to the amplitude of the tail current. $[K^+]_o$ was 150 mM.

course of the deactivation. The resultant traces in the lower row of Fig. 8*A* show that the amplitude of the 'hook' becomes larger with stronger depolarization and yet the time constants appear to be constant.

Possible causes of this phenomenon may include an activation of some other current, unblocking of the channel, or removal of an inactivated component of I_K.

The Na^+–Ca^{2+} exchange current or Na^+–K^+ pump current can be excluded because experiments were done in a $[K^+]_o$ of 150 mM, a $[K^+]_i$ of 150 mM and in the absence of Na^+. The hyperpolarization-activated inward current (I_f or I_h) has a much slower time course and smaller amplitude at these potential ranges. Since the 'hook' of I_K was also seen in the same voltage range at a $[K^+]_o$ of 50 mM (not illustrated in the Figure) as at a $[K^+]_o$ of 150 mM, the blocking of the channel with Na^+ or K^+ during depolarization and its unblocking on hyperpolarization are also considered unlikely. The most plausible explanation would thus appear to be that a fraction of I_K is partially inactivated during the depolarization, and on hyperpolarization this inactivation is removed with a fast time course, which gives rise to a 'hook'.

To test whether this 'hook' of the tail current is due to the I_K channel, the initial part of the ensemble average current was examined by carefully subtracting the capacitive transient from each original current record (Fig. 8*B*). The ensemble average current, reconstructed from 156 idealized single-channel current traces, suggested the presence of an initial downward deflexion of the average current. This confirmed that the 'hook' of the whole-cell current tail is due to the properties of I_K itself and not an overlap of other currents.

The time course of the inactivation process could not be resolved during depolarization, but it could be demonstrated by recording the inward tail current generated by varying the duration of the preceding depolarizing pulses (Fig. 8*C*). The membrane was first depolarized from a holding potential of −43 mV to +7 mV for various durations and then repolarized to −73 mV. The 'hook' of the tail current on repolarization was detectable even after a depolarizing pre-pulse shorter than 20 ms. In the lower row of Fig. 8*C*, the ratio of the quasi-instantaneous current level to the amplitude of the tail current measured by the same method as shown in the lower row of Fig. 8*A* was plotted against time. The time course of this ratio could indicate the evolution of the inactivation. This finding indicates that a fraction of I_K is inactivated very quickly as the membrane is depolarized.

Slow decay of the macroscopic current

During sustained depolarization above 0 mV, the outward macroscopic current decayed slowly. Fig. 9 shows the activation of I_K on depolarization to +7 mV for various durations followed by hyperpolarization to yield the envelope curves at −43 mV in a $[K^+]_o$ of 5·4 mM (*A*) and at −73 mV in a $[K^+]_o$ of 50 mM (*B*) and a $[K^+]_o$ of 150 mM (*C*). Both the current on depolarization and the envelope initially increased, and then declined slowly with a similar time course. More than 500 ms was required to reach a steady state. The time constant of the slow decay varied between 400 and 800 ms in five cells. In the steady state, the current amplitude decreased to 54 or 88 % of the peak amplitude. This slow change in the current could not be the same inactivation which was removed quickly by hyperpolarization as mentioned above for the following two reasons. (1) The slow decay during depolarization occurred with a time constant in excess of 400 ms but the 'hook' on repolarization was detectable even after preceding depolarization of less than 20 ms (Fig. 8*C*). (2) The slow decay was observed only when the membrane was depolarized above 0 mV,

and not at −23 or −13 mV, yet the 'hook' was observed upon subsequent repolarization.

The slow decay of the macroscopic current during strong depolarization may result from a slow inactivation of I_K itself, from a positive shift of the K^+ equilibrium potential, E_K, during I_K activation, or from an overlap of another K^+ current. A positive shift of E_K might arise from K^+ accumulation near the outer surface of the

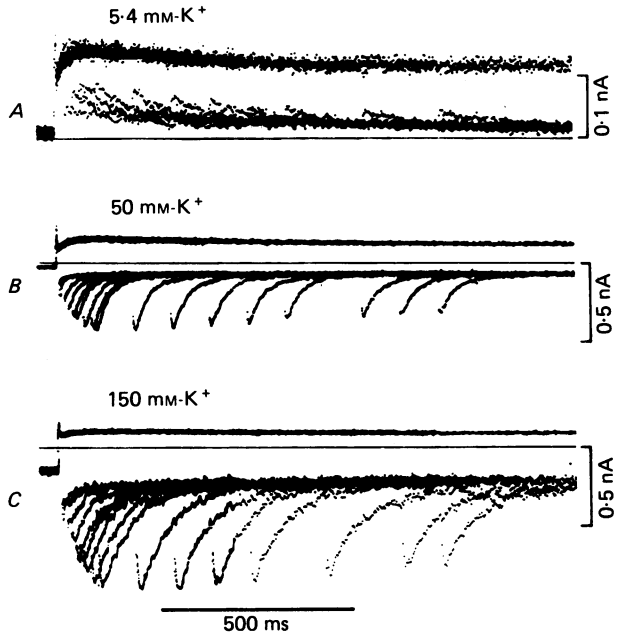

Fig. 9. Slow decay of the macroscopic current following activation of I_K during sustained depolarization. In this protocol, depolarizing pulses of various durations from a holding potential of −43 mV to +7 mV were applied, and this was followed by hyperpolarizing pulses to −43 mV in a $[K^+]_o$ of 5·4 mM (*A*), or to −73 mV in a $[K^+]_o$ of 50 mM (*B*) or a $[K^+]_o$ of 150 mM (*C*). Current records were superimposed. The envelope curve was obtained by connecting the peak of the currents on repolarization. Note that the time course of the onset of the current and the time course of the envelope curve are very similar. The time constants of slow decay were 460 ms at a $[K^+]_o$ of 5·4 mM, 440 ms at 50 mM, and 470 ms at 150 mM, respectively.

membrane or from K^+ depletion at the inner surface. The positive shift of E_K might explain the slow decay of the current during depolarization, but it cannot account for the gradual decline of the envelope curve when the membrane was clamped back from potentials positive to E_K to potentials negative to E_K (Fig. 9*B* and *C*). Decay may also occur if the transient outward current, having a reversal potential of −40 mV (Nakayama & Irisawa, 1985), is inactivated during depolarization. This possibility is, however, considered unlikely, since slow decay also occurs in the envelope curve at −43 mV in a $[K^+]_o$ of 5·4 mM, where the transient outward current is not seen. It seems most likely therefore that I_K itself slowly inactivates, although the possibility of the presence of some other current cannot be entirely excluded.

Inward rectification of I_K

In the cell-attached patch mode, it was not possible to identify the outward current of the single delayed rectifier K^+ channel because strong depolarizations frequently destroyed the gigaseal and furthermore I_K seemed to be inactivated. Thus, at potentials positive to E_K, the conductance and kinetics of I_K had to be estimated using the whole-cell current record.

In Fig. 6*A*, the membrane was hyperpolarized to various levels after constant depolarization to +7 mV. The amplitudes of the tail currents (ΔI_K) were measured by extrapolating the time course towards the end of the preceding pulse. The time-dependent change (ΔI_K) of the current can be expressed as:

$$\Delta I_K = (p_a^0 - p_a^\infty)\, p_i^\infty\, \bar{I}_K, \tag{4}$$

where p_a^0 and p_a^∞ are the initial and steady-state values of the open probability in the activation gate and p_i^∞ is the steady-state value of the open probability in the quick inactivation process. $\bar{I}_K$ means fully activated, non-inactivated I_K which is defined as:

$$\bar{I}_K = N\gamma(E - E_K), \tag{5}$$

where γ is assumed to be voltage independent and N is the total number of channels per cell. On rearranging eqn. (4),

$$p_i^\infty\, \bar{I}_K = \frac{\Delta I_K}{(p_a^0 - p_a^\infty)}. \tag{6}$$

ΔI_K was determined as the current change either during depolarizing pulses as shown in Fig. 1, or during the second pulse of the double-pulse experiment as shown in Fig. 6*A*. Values of $(p_a^0 - p_a^\infty)$ were calculated using eqn. (1). The relation between the $p_i^\infty\, \bar{I}_K$ values obtained from eqn. (6), and the membrane potential revealed an intense inward-going rectification of the current (Fig. 10).

The chord conductance was decreased with depolarization within a wide range between −100 and +30 mV, regardless of $[K^+]_o$. Since the single-channel conductance of I_K was constant, at least in the potential range negative to E_K, p_i^∞ was considered to cause inward rectification of I_K. Thus, the inward-going rectification may be due to rapid closure of a significant population of I_K channels immediately after the onset of depolarization.

Kinetics of the fast inactivation gate

The kinetics of the fast inactivation gate were calculated on the basis of the histogram shown in Fig. 7. At potentials more negative than the threshold of I_K activation (−50 mV), the open rate constant of the activation gate (α_a) can be assumed to be zero. Thus, the open and closed rate constants (α_i and β_i) of the fast inactivation gate can be calculated from the following equations (see Appendix):

$$\alpha_i = \tfrac{1}{2}(1/\tau_{slow} + 1/\tau_{fast} - 1/\tau_{open}), \tag{7}$$

$$\beta_i = 1/\tau_{open} - \beta_a, \tag{8}$$

where β_a is the closed rate constant of the activation gate. Values of τ_{slow}, τ_{fast} and τ_{open} were obtained from Fig. 7*B*. Fig. 11*A* shows plots of α_i and β_i against the

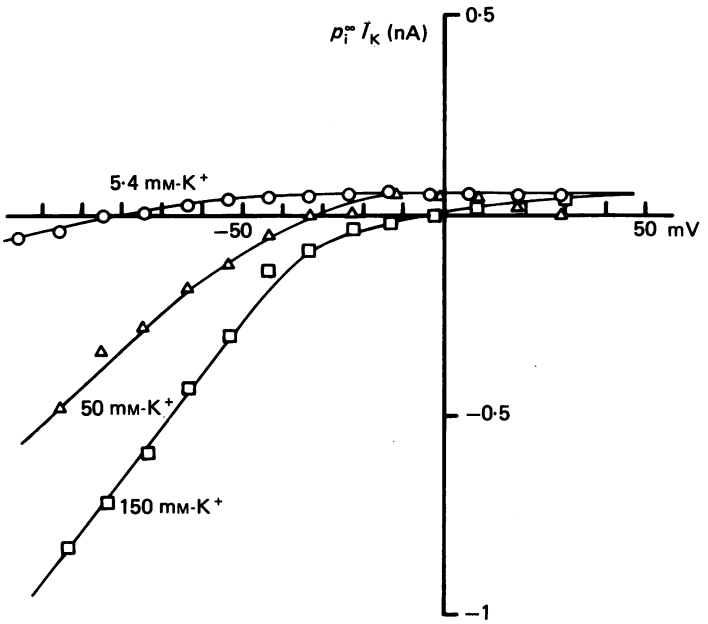

Fig. 10. Relation between $p_i^\infty \bar{I}_K$ and the membrane potential, revealing an intense inward-going rectification. The chord conductance of the macroscopic current was decreased with depolarization within a wide range between −100 and +30 mV, regardless of $[K^+]_o$. $[K^+]_o$ (in mM): ○, 5·4; △, 50; □, 150.

membrane potential. From the regression lines, the rate constants were determined as follows:

$$\alpha_i = 100 \exp(-0{\cdot}0183\, E), \tag{9}$$

$$\beta_i = 656 \exp(0{\cdot}00942\, E). \tag{10}$$

These relations indicate that the open rate constant decreases and the closed rate constant increases upon depolarization, and consequently this gate closes at more positive potentials. The open probability of the inactivation gate in the steady state (p_i^∞) is expressed by the following equation:

$$p_i^\infty = \alpha_i/(\alpha_i + \beta_i). \tag{11}$$

The continuous curve in Fig. 11*B* demonstrates the relation between p_i^∞ and the membrane potential. The value of p_i^∞ is assumed to be 0·5 at −68 mV where α_i is equal to β_i (Fig. 11*A*).

In order to evaluate the inactivation curve from the macroscopic current, the chord conductances obtained from Fig. 10 were normalized with respect to those at −63 mV where the absolute value of the chord conductance can be assumed to be 0·5 (Fig. 11*B*). The values of p_i^∞ obtained in the two different ways were very similar (Fig. 11*B*). The slope of the open probability of the inactivation gate was much less steep than the slope of the activation curve (cf. Fig. 2*B*).

In the case of Fig. 10, the value of $p_i^\infty \bar{I}_K$ was 0·43 nA at −63 mV in a $[K^+]_o$ of 150 mM. Since p_i^∞ was assumed to be 0·5, $\bar{I}_K$ was estimated as 0·86 nA. Using eqn.

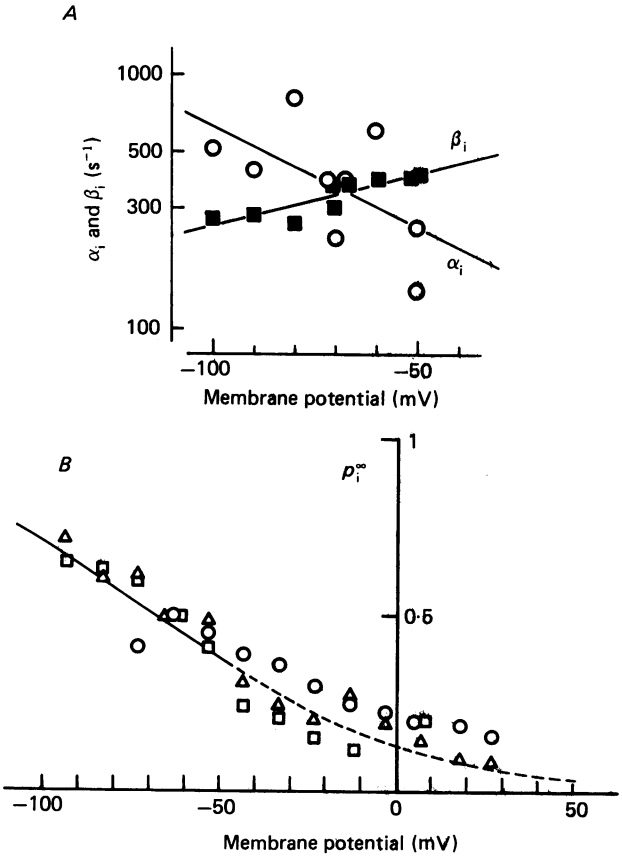

Fig. 11. *A*, voltage dependence of the open and closed rate constants of the inactivation gate (α_i (○); β_i (■)). The rate constants were calculated on the basis of the kinetic model of I_K as described in the Appendix. Lines were drawn by the least-squares method. *B*, inactivation curve of I_K. The symbols indicate the values of p_i^∞ obtained by normalizing the chord conductance of $p_i^\infty I_K$ shown in Fig. 10. The continuous line was drawn on the basis of the value of $\alpha_i/(\alpha_i+\beta_i)$ where α_i and β_i were calculated from eqns. (9) and (10), respectively. The interrupted line was drawn by assuming that eqns. (9) and (10) could be applied to potentials positive to −50 mV. Note that the p_i^∞ values obtained in the two different ways coincided very well.

(5), the value of N, the number of channels per cell, was therefore calculated as 1230 (1054 ± 284, $n = 13$).

DISCUSSION

Single-channel conductance of I_K

One of the major findings in the present study was that the single-channel conductance of I_K, γ, was as small as 1·6 pS in the physiological 5·4 mM-K^+ solution. The above small value may represent one of the reasons why the unitary current of I_K had not been recorded in pace-maker cells. The value is one-fourth of that of inward rectifier K^+ channels in ventricular cells (Kameyama, Kiyosue & Soejima, 1983; Sakmann & Trube, 1984*a*) and is similar to that of the delayed rectifier K^+

channel obtained by noise analysis in snail neurones (2·4 pS, Reuter & Stevens, 1980). A single-channel K^+ conductance of 17·5 pS has been reported in squid axons (Conti & Neher, 1980), which is higher than the value obtained in this experiment, but this difference may reflect the different composition of their bathing solution (460 mM-extracellular K^+–1 mM-intracellular K^+). In the frog skeletal muscle (Standen, Stanfield & Ward, 1985) the values of γ were 15 pS in a $[K^+]_o$ of 2·5 mM, 24 pS in a $[K^+]_o$ of 60 mM and 30 pS in a $[K^+]_o$ of 120 mM, respectively. The delayed rectifier K^+ channel in the skeletal muscle cell is thus less sensitive to $[K^+]_o$ than that in the cardiac pace-maker cell. A large single-channel conductance of more than 60 pS (4·0 mM-extracellular K^+–140 mM-intracellular K^+) has been reported for the chick embryo ventricle (Clapham & DeFelice, 1984), which is very different from the present data. The single-channel conductance of cardiac pace-maker cells may be smaller than that in other tissues.

The total number of I_K channels was estimated at about 1000 per cell. Assuming the surface area of a nodal cell to be 1400 μm^2 (Nakayama *et al.* 1984), the channel density is estimated at 0·7 channels/μm^2, which is approximately similar to that of inward-rectifier K^+ channels (Sakmann & Trube, 1984*a*), and of ATP-regulated K^+ channels in ventricular cells (Kakei, Noma & Shibasaki, 1985; Noma & Shibasaki, 1985).

Time course of activation of I_K

The bell-shaped relation between the time constant of activation and the membrane potential had been predicted by simulation studies. At negative membrane potentials, it had not been possible to measure the time constants in multicellular preparations, due to the interference of I_h (or I_f) (DiFrancesco *et al.* 1979; Yanagihara & Irisawa, 1980). The rate constants, α_a and β_a, calculated at 10 mV in the present experiment were 25·2 and 0·2 s^{-1}, respectively. Values close to these were used in Noble & Noble's simulation (1984), i.e. 16·0 and 0·8 s^{-1}, respectively. Yanagihara, Noma & Irisawa (1980) obtained slightly smaller values of 7·8 and 0·3 s^{-1}, respectively. This difference may reflect the different types of preparations. In multicellular specimens, K^+ is likely to accumulate in the extracellular space due to the outward K^+ current, which could possibly reduce the amplitude of I_K and result in an apparent retardation of the time course of I_K activation. Larger series resistance may also be an additional factor in the slow rate constant of multicellular specimens. For these reasons, the activation of I_K in Yanagihara *et al.*'s simulation (1980) is probably underestimated. When they reconstructed the action potential of pace-maker cells based on their voltage-clamp experiments, they had to assume a large outward leak current during depolarization, because activation of I_K was too small to bring about repolarization of the membrane. The faster rate constant obtained in the present study ensures that activation of I_K is sufficient to repolarize the membrane.

At potentials negative to −30 mV, the time constants in a $[K^+]_o$ of 50 mM are shorter than those in a $[K^+]_o$ of 5·4 or 150 mM (Fig. 6). Since these potentials are negative to E_K in an extracellular solution which contained 50 mM-K^+ and 100 mM-Na^+, the shorter time constant could be due to a blocking effect of extracellular Na^+ on the inward current of I_K.

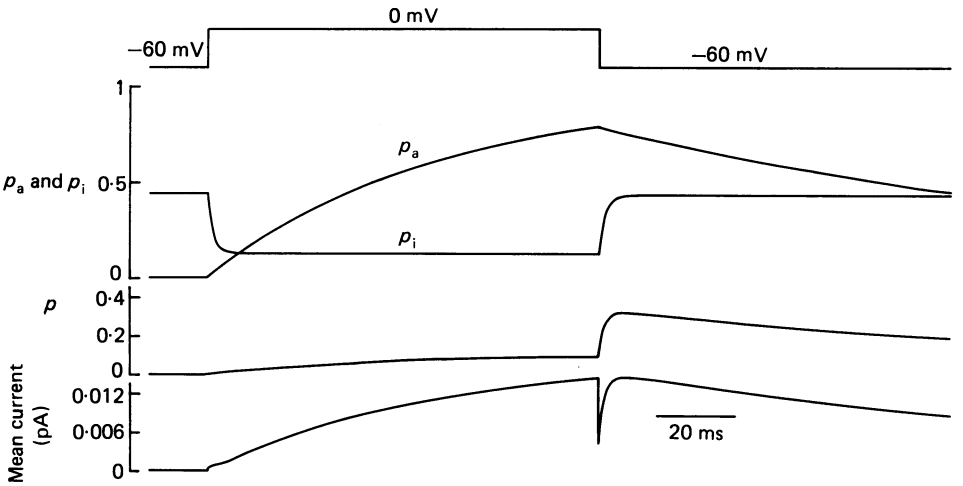

Fig. 12. Simulation of the time course of three kinds of open probabilities and the mean current through the single channel at a $[K^+]_o$ of 5·4 mM. The probabilities of the activation gate, of the inactivation gate and of the channel opening are denoted as p_a, p_i and p, respectively. The clamp pulse was from −60 to 0 mV for 100 ms. During the depolarization, the values of p_a and p_i could be expressed as:

$$p_a = 0{\cdot}967 + (0{\cdot}008 - 0{\cdot}967) \exp(-t/58),$$

$$p_i = 0{\cdot}132 + (0{\cdot}445 - 0{\cdot}132) \exp(-t/1{\cdot}3),$$

where time, t, is in milliseconds. During the repolarization, they were

$$p_a = 0{\cdot}008 + (0{\cdot}795 - 0{\cdot}008) \exp(-t/165),$$

$$p_i = 0{\cdot}445 + (0{\cdot}132 - 0{\cdot}445) \exp(-t/1{\cdot}5).$$

Fast inactivation and inward rectification

I_K has an inward-going rectification in the 'fully activated' I–V relation (Noma & Irisawa, 1976; DiFrancesco *et al.* 1979; Yanagihara & Irisawa, 1980). This rectification can be attributed to the fast inactivation gate found in the present study. The removal phase of the fast inactivation had not been recorded in multicellular specimens, probably because of a large series resistance and the resultant slow decay of the capacitive current in such preparations. In this study, the author used single pace-maker cells with a relatively rapid capacitive surge and a high signal-to-noise ratio of the inward current tail at high $[K^+]_o$. The time course of the removal of inactivation was too fast to permit quantitative evaluation in the case of the macroscopic current, and the kinetics of the inactivation gate of I_K was therefore evaluated by single-channel analysis.

A possible alternative interpretation of the 'hook' in the macroscopic I_K is an activation of the inward-rectifier K^+ current ($I_{K,rec}$ or I_{K1}) since $I_{K,rec}$ is activated with hyperpolarization (Kurachi, 1985). This possibility, however, can be excluded since the inward-rectifier K^+ channels were rarely recorded in the nodal cells (Noma, Nakayama, Kurachi & Irisawa, 1984). In addition, the 'hook' was observed regardless of $[K^+]_o$, since activation and inactivation kinetics of I_K depend only on the membrane potential (Figs. 2 and 11), whereas those of $I_{K,rec}$ depend on both the

membrane potential and $[K^+]_o$ (Kameyama *et al.* 1983; Sakmann & Trube, 1984*b*; Kurachi, 1985). It is therefore unlikely that $I_{K,rec}$ participates in the inward rectification of the macroscopic I_K.

Physiological significance of the inactivation gate in the pace-maker potential

Fig. 12 shows a reconstructed voltage-clamp experiment, with various parameters such as the open probability of the activation gate (p_a), open probability of the inactivation gate (p_i), open probability of the channel (p) and the mean current through the single channel at a $[K^+]_o$ of 5·4 mM. The clamp pluse is from −60 to 0 mV for 100 ms. During the depolarization, p_a progressively increases with a time constant of 58 ms, which is followed by a slow deactivation with $\tau_a = 165$ ms on repolarization. On the other hand, p_i rapidly decreases ($\tau_i = 1{\cdot}3$ ms) upon depolarization, and upon repolarization the inactivation is removed at a rapid rate of $\tau_i = 1{\cdot}5$ ms. The probability of the channel opening (p) is the product of p_a and p_i, so that p remains very small at 0 mV, whereas it increases suddenly upon repolarization to −60 mV due to the removal of the inactivation. In spite of this large change in p, the value of the amplitude of the mean current is not very different at the end of the depolarization compared with that at the beginning of the repolarization. This is because even though p is small at 0 mV the driving force in a $[K^+]_o$ of 5·4 mM is large, while at −60 mV p is large, but the driving force is small. This may be one of the crucial points of the mechanism whereby it is possible for I_K to be involved in the pace-maker depolarization.

APPENDIX

To interpret the time course of I_K, two independent gates (i.e. an activation gate and an inactivation gate) are assumed. In this assumption, the slow decay of the macroscopic current, as illustrated in Fig. 9, is ignored because of its extremely slow time course and unknown nature. Each process can be described as a first-order transition between open and closed states or between non-inactivated and inactivated states:

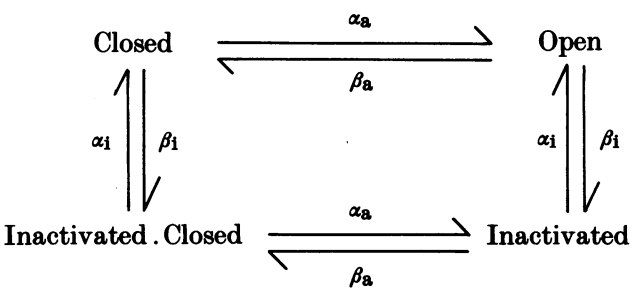

where α_a and α_i are the opening rate constants and β_a and β_i are the closing rate constants, which depend on the membrane potential but not on $[K^+]_o$. The macroscopic current of I_K can be described by the expression:

$$I_K = p_a p_i N i, \tag{12}$$

where p_a and p_i are the open probabilities of the activation gate and of the inactivation gate, i is the unit amplitude of the single-channel current and N is the

total number of channels within the cell, respectively. Each open probability can be expressed as:

$$p_a = p_a^\infty + (p_a^0 - p_a^\infty) \exp(-t/\tau_a), \tag{13}$$

$$p_i = p_i^\infty + (p_i^0 - p_i^\infty) \exp(-t/\tau_i), \tag{14}$$

where p_a^0, p_i^0, p_a^∞, p_i^∞ are the initial and steady-state values, respectively. The time constants are

$$\tau_a = 1/(\alpha_a + \beta_a), \tag{15}$$

$$\tau_i = 1/(\alpha_i + \beta_i). \tag{16}$$

The open probabilities of the activation and inactivation gates in the steady state can be expressed as:

$$p_a^\infty = \alpha_a/(\alpha_a + \beta_a), \tag{17}$$

$$p_i^\infty = \alpha_i/(\alpha_i + \beta_i). \tag{18}$$

The probability density functions of the open time, $f_{o(t)}$, and the closed time, $f_{c(t)}$, are

$$f_{o(t)} = (\beta_a + \beta_i) \exp\{-(\beta_a + \beta_i)t\}, \tag{19}$$

and

$$f_{c(t)} = A \exp(-\lambda_1 t) + B \exp(-\lambda_2 t) + \lambda_3 C \exp(-\lambda_3 t), \tag{20}$$

where A, B and $\lambda_3 C$ are the constants measured at the crossing point where the three components of the closed-time histogram meet the probability axis (at $t = 0$), $C = (1 - A/\lambda_1 - B/\lambda_2)$ and λ_1, λ_2 and λ_3 ($\lambda_1 > \lambda_2 > \lambda_3 > 0$) are the solutions of the following simultaneous equations:

$$\lambda_1 + \lambda_2 + \lambda_3 = 2(\alpha_a + \alpha_i) + (\beta_a + \beta_i), \tag{21}$$

$$\lambda_1\lambda_2 + \lambda_2\lambda_3 + \lambda_3\lambda_1 = \alpha_a^2 + \alpha_a\beta_a + 3\alpha_a\alpha_i + \alpha_a\beta_i + \beta_a\alpha_i + \beta_a\beta_i + \alpha_i^2 + \alpha_i\beta_i, \tag{22}$$

$$\lambda_1\lambda_2\lambda_3 = \alpha_a\alpha_i(\alpha_a + \beta_a + \alpha_i + \beta_i). \tag{23}$$

For simplicity, we assume that α_a is zero at potentials negative to -50 mV, so that λ_3 is also zero by using eqn. (23). Thus,

$$f_{c(t)} = A \exp(-\lambda_1 t) + B \exp(-\lambda_2 t). \tag{24}$$

The channel therefore has one exponential component for the open time and two exponential components for the closed time at potentials negative to -50 mV. In the open- and closed-time histograms, τ_{open}, τ_{slow} and τ_{fast} correspond to $(\beta_a + \beta_i)^{-1}$, λ_2^{-1} and λ_1^{-1}, respectively. The rate constants at potentials negative to -50 mV can be calculated from the present experimental data:

$$\alpha_a = \frac{p_a^\infty}{\tau_a}, \tag{25}$$

$$\beta_a = \frac{1}{\tau_a}. \tag{26}$$

From eqn. (21),

$$\alpha_i = \frac{1}{2}\left(\frac{1}{\tau_{slow}} + \frac{1}{\tau_{fast}} - \frac{1}{\tau_{open}}\right), \tag{27}$$

$$\beta_i = \frac{1}{\tau_{open}} - \beta_a. \tag{28}$$

The author wishes to thank Professor H. Irisawa, Professor A. Noma, Dr M. Kameyama and Dr J. Kimura for their invaluable advice and continuous encouragement at all stages of this study. Acknowledgement is also due to Professor S. Hirakawa, Gifu University School of Medicine, for providing me with an opportunity to work at the National Institute for Physiological Sciences. This study was performed with expert technical assistance from Mr M. Ohara and Mr O. Nagata.

REFERENCES

BROWN, H. F. (1982). Electrophysiology of the sinoatrial node. *Physiological Reviews* **62**, 505–530.

BROWN, H. F., GILES, W. R. & NOBLE, S. J. (1977). Membrane currents underlying activity in frog sinus venosus. *Journal of Physiology* **271**, 783–816.

BROWN, H. F., KIMURA, J. & NOBLE, S. J. (1982). The relative contributions of various time-dependent membrane currents to pacemaker activity in the sino-atrial node. In *Cardiac Rate and Rhythm*, ed. BOUMAN, L. N. & JONGSMA, H. J., pp. 53–68. The Hague: Martinus Nijhoff.

CLAPHAM, D. E. & DEFELICE, L. J. (1984). Voltage-activated K channels in embryonic chick heart. *Biophysical Journal* **45**, 40–42.

CONTI, F. & NEHER, E. (1980). Single channel recordings of K^+ currents in squid axons. *Nature* **285**, 140–143.

DIFRANCESCO, D., NOMA, A. & TRAUTWEIN, W. (1979). Kinetics and magnitude of the time-dependent potassium current in the rabbit sinoatrial node. *Pflügers Archiv* **381**, 271–279.

FUKUSHIMA, Y. (1982). Blocking kinetics of the anomalous potassium rectifier of tunicate egg studied by single channel recording. *Journal of Physiology* **331**, 311–331.

GILES, W. R. & SHIBATA, E. F. (1985). Voltage clamp of bull-frog cardiac pace-maker cells: a quantitative analysis of potassium currents. *Journal of Physiology* **368**, 265–292.

HAGIWARA, S. & TAKAHASHI, K. (1974). The anomalous rectification and cation selectivity of the membrane of a starfish egg cell. *Journal of Membrane Biology* **18**, 61–80.

HAMILL, O. P., MARTY, A., NEHER, E., SAKMANN, B. & SIGWORTH, F. J. (1981). Improved patch-clamp techniques for high-resolution current recording from cells and cell-free membrane patches. *Pflügers Archiv* **391**, 85–100.

IRISAWA, H. (1978). Comparative physiology of the cardiac pacemaker mechanism. *Physiological Reviews* **58**, 461–498.

ISENBERG, G. & KLÖCKNER, U. (1982). Calcium-tolerant ventricular myocytes prepared by preincubation in a 'KB Medium'. *Pflügers Archiv* **395**, 6–18.

KAKEI, M. & NOMA, A. (1984). Adenosine-5′-triphosphate-sensitive single potassium channel in the atrioventricular node cell of the rabbit heart. *Journal of Physiology* **352**, 265–284.

KAKEI, M., NOMA, A. & SHIBASAKI, T. (1985). Properties of adenosine-triphosphate-regulated potassium channels in guinea-pig ventricular cells. *Journal of Physiology* **363**, 441–462.

KAMEYAMA, M., KIYOSUE, T. & SOEJIMA, M. (1983). Single channel analysis of the inward rectifier K current in the rabbit ventricular cells. *Japanese Journal of Physiology* **33**, 1039–1056.

KOKUBUN, S., NISHIMURA, M., NOMA, A. & IRISAWA, H. (1982). Membrane currents in the rabbit atrioventricular node cell. *Pflügers Archiv* **393**, 15–22.

KURACHI, Y. (1985). Voltage-dependent activation of the inward-rectifier potassium channel in the ventricular cell membrane of guinea-pig heart. *Journal of Physiology* **366**, 365–385.

MATSUDA, H. & NOMA, A. (1984). Isolation of calcium current and its sensitivity to monovalent cations in dialysed ventricular cells of guinea-pig. *Journal of Physiology* **357**, 553–573.

NAKAMURA, S., HAMA, K., ASAI, J. & IRISAWA, H. (1986). Observations on the fine structure of nodal, Purkinje and working myocardial cells isolated from rabbit hearts. *Archivum histologicum japonicum* **49**, 105–116.

NAKAYAMA, T. & IRISAWA, H. (1985). Transient outward current carried by potassium and sodium in quiescent atrioventricular node cells of rabbits. *Circulation Research* **57**, 65–73.

NAKAYAMA, T., KURACHI, Y., NOMA, A. & IRISAWA, H. (1984). Action potential and membrane currents of single pacemaker cells of the rabbit heart. *Pflügers Archiv* **402**, 248–257.

NOBLE, D. & NOBLE, S. J. (1984). A model of sino-atrial node electrical activity based on a modification of the DiFrancesco–Noble (1984) equations. *Proceedings of Royal Society* B **222**, 295–304.

NOMA, A. & IRISAWA, H. (1976). A time- and voltage-dependent potassium current in the rabbit sinoatrial node cell. *Pflügers Archiv* **366**, 251–258.

NOMA, A., KOTAKE, H. & IRISAWA, H. (1980). Slow inward current and its role mediating the chronotropic effect of epinephrine in the rabbit sinoatrial node. *Pflügers Archiv* **388**, 1–9.

NOMA, A., NAKAYAMA, T., KURACHI, Y. & IRISAWA, H. (1984). Resting K conductances in pacemaker and non-pacemaker heart cells of the rabbit. *Japanese Journal of Physiology* **34**, 245–254.

NOMA, A. & SHIBASAKI, T. (1985). Membrane current through adenosine–triphosphate-regulated potassium channels in guinea-pig ventricular cells. *Journal of Physiology* **363**, 463–480.

REUTER, H. & STEVENS, C. F. (1980). Ion conductance and ion selectivity of potassium channels in snail neurones. *Journal of Membrane Biology* **57**, 103–118.

SAKMANN, B., NOMA, A. & TRAUTWEIN, W. (1983). Acetylcholine activation of single muscarinic K^+ channels on isolated pacemaker cells of the mammalian heart. *Nature* **303**, 250–253.

SAKMANN, B. & TRUBE, G. (1984*a*). Conductance properties of single inwardly rectifying potassium channels in ventricular cells from guinea-pig heart. *Journal of Physiology* **347**, 641–657.

SAKMANN, B. & TRUBE, G. (1984*b*). Voltage-dependent inactivation of inward-rectifying single-channel currents in the guinea-pig heart cell membrane. *Journal of Physiology* **347**, 659–683.

SOEJIMA, M. & NOMA, A. (1984). Mode of regulation of the ACh-sensitive K-channel by the muscarinic receptor in rabbit atrial cells. *Pflügers Archiv* **400**, 424–431.

STANDEN, N. B., STANFIELD, P. R. & WARD, T. A. (1985). Properties of single potassium channels in vesicles formed from the sarcolemma of frog skeletal muscle. *Journal of Physiology* **364**, 339–358.

TANIGUCHI, J., KOKUBUN, S., NOMA, A. & IRISAWA, H. (1981). Spontaneously active cells isolated from the sino-atrial and atrio-ventricular nodes of the rabbit heart. *Japanese Journal of Physiology* **31**, 547–558.

YANAGIHARA, K. & IRISAWA, H. (1980). Potassium current during the pacemaker depolarization in rabbit sinoatrial node cell. *Pflügers Archiv* **388**, 255–260.

YANAGIHARA, K., NOMA, A. & IRISAWA, H. (1980). Reconstruction of sino-atrial node pacemaker potential based on the voltage clamp experiments. *Japanese Journal of Physiology* **30**, 841–857.